Aalto University

OPEN ACCESS

This is an electronic reprint of the original article.
This reprint may differ from the original in pagination and typographic detail.

Ilter, Mehmet; Vehkaperä, Mikko; Wichman, Risto; Hämäläinen, Jyri

Coded transmission under non-cooperative radar interference

Published in:
2020 IEEE International Conference on Communications Workshops, ICC Workshops 2020 - Proceedings

DOI:
10.1109/ICCWorkshops49005.2020.9145191

Published: 01/06/2020

Document Version
Peer-reviewed accepted author manuscript, also known as Final accepted manuscript or Post-print

Please cite the original version:
Ilter, M., Vehkaperä, M., Wichman, R., & Hämäläinen, J. (2020). Coded transmission under non-cooperative radar interference. In *2020 IEEE International Conference on Communications Workshops, ICC Workshops 2020 - Proceedings* Article 9145191 IEEE. https://doi.org/10.1109/ICCWorkshops49005.2020.9145191

This material is protected by copyright and other intellectual property rights, and duplication or sale of all or part of any of the repository collections is not permitted, except that material may be duplicated by you for your research use or educational purposes in electronic or print form. You must obtain permission for any other use. Electronic or print copies may not be offered, whether for sale or otherwise to anyone who is not an authorised user.

Coded Transmission Under Non-Cooperative Radar Interference

Mehmet Cagri Ilter*, Mikko Vehkaperä‡, Risto Wichman*, and Jyri Hämäläinen†

* Department of Signal Processing and Acoustics, Aalto University, Espoo, Finland
‡VTT Technical Research Centre of Finland, Oulu, Finland
†Department of Communications and Networking, Aalto University, Espoo, Finland
e-mail:{mehmet.ilter, risto.wichman, jyri.hamalainen}@aalto.fi
mikko.vehkapera@vtt.fi

***Abstract*—There has been increasing interest for the coexistence of communication and radar systems which share the same wireless channel. This paper investigates the effect of non-cooperative additive radar interference for a communication channel where convolutional encoder is used. In order to include any given pair of convolutional encoder and M-ary constellation in the analysis, bit-error-rate (BER) bound expressions for low and high interference regions are derived based on product-state matrix technique. Thus, the any chosen constellation together with convolutional encoder does not need to satisfy the quasi-regularity (QR) property that includes geometrical uniformity and symmetry. Numerical results validate the derived performance bounds and using proper optimization techniques, the derived expressions can be utilized in search for good constellations for a given coding scheme suffering from radar interference without any restrictions on the constellation points and the choice of convolutional encoder.**

I. Introduction

Wireless communications systems operating on the frequency bands that are currently allocated solely to radar systems have recently gained interest due to the congestion experienced by the cellular systems in sub-6 GHz frequencies [1]. Ideally such co-existing systems would be jointly designed so that the mutual interference is minimized and performance maximized [2]. This would, however, require a complete re-design and replacement of the existing systems, so a more practical scenario is the one where the radar and communication systems are designed in isolation and operate with minimal knowledge of each other.

The performance of wireless communication systems coexisting with non-cooperative radars that transmit unaltered signals has been analyzed in some recent works [3], [4]. More precisely, in [3], [5], the uncoded symbol error rate (SER) was calculated for AWGN channels suffering from additive radar interference (ARI) while [4] considered the capacity analysis of the same channel. To the best of our knowledge, however, the performance of communication systems employing practical forward error correction coding under ARI has been evaluated only for binary modulation via computer simulations [6] and the performance of coded transmission with irregular constellation, where any regular grid constraint on constellation points does not exist, under ARI has not been addressed yet.

Considering short packet transmission in 5G and beyond 5G networks, a convolutional encoder can be preferred over capacity-approaching error correcting codes [7] where the latter ones cannot tackle desired latency requirements due to their iterative decoding process [8]. For instance, it was interestingly shown that even polar codes have became less preferable than convolutional encoders in particular packet size and system complexity requirements [9].

Error performance analysis of error correcting codes is typically based on the assumption that their performance is independent of the transmitted sequence. While this is true for quasi-regular (QR) cases, many systems are in fact irregular; especially for when the encoders are paired with non-uniformly spaced constellations [10]. For the communication systems suffering from non-cooperative radar interference, the optimal irregular constellations have been proposed in [11] for uncoded scenarios by utilizing deep learning techniques. Interestingly, this can be also observed in the cases where a convolutional encoder used with conventional M-QAM and M-PSK constellations [10].

Motivated by this fact, this paper investigates the error performance of convolutionally coded communication system for any given pair of the convolutional encoder and the constellation over AWGN channels under ARI. To the best our knowledge, this paper provides the first example of deploying a convolutional encoder with any given M-ary constellation with the existence of non-cooperative additive radar interference. In order to encompass QR and irregular scenarios in the performance analysis for any given convolutional encoder along with any type of constellation, the general error performance analysis is represented, where the product-state matrix technique is utilized for the first time over ARI cases.

The rest of the paper is organized as follows. The system model for convolutionally coded transmission with ARI is described in Section II. Error performance analysis, including generating function calculation via the product-state matrix technique and its derivations for both low-INR and high-INR regions, are given in Section III. Derived BER bound expressions are compared to simulation results in Section IV, and Section V completes the paper with concluding remarks.

II. System Model

The system model of the convolutionally coded transmission with the existence of additive radar interference is shown in Fig. 1. Specifically, the information bits of a given frame, $\mathbf{b}$,

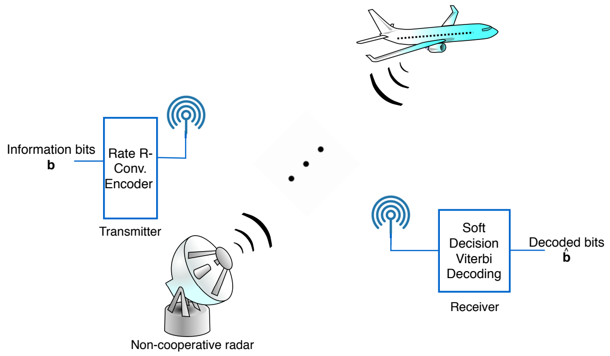

Fig. 1: Convolutionally coded transmission model with the existence of non-cooperative radar interference.

are encoded by a rate R-convolutional encoder and the encoded bits are fed to the bit-to-symbol mapper where the transmitting symbols are generated from a M-ary constellation, $\{x_i\}_{i=1}^{M}$, with average energy of $\mathcal{S}$ in the transmitter. Then, the received signal after one symbol duration can be expressed as

$$y = \sqrt{\mathcal{S}}x + \sqrt{\mathcal{I}}e^{-j\theta} + Z, \tag{1}$$

where x is a constellation point mapped to the corresponding information bit(s) and $\sqrt{\mathcal{I}}e^{-j\theta}$ is the amplitude-constant additive radar signal as in [5]. Here, $\mathcal{I}$ can be considered as the average INR resulting from the radar interference after assuming Z is a zero-mean unit-variance proper-complex Gaussian noise. Also, θ denotes the random phase component of the interfering radar signal which has a uniform distribution over $[0, 2\pi)$.

In order to decode transmitted symbol in the receiver, soft-decision Viterbi decoding is utilized in which optimal MAP receiver is implemented for possible transition probabilities during a frame. More explicitly, the optimal MAP rule under non-cooperative radar interference is given by [5]:

$$\arg \min_{k\in\{1,\cdots,M\}} \mathbb{E}_\theta \left[|y - \sqrt{\mathcal{S}}x_k|^2 - \ln \mathcal{I}_0 \left(2\sqrt{\mathcal{I}}|y - \sqrt{\mathcal{S}}x_k| \right) \right]. \tag{2}$$

Here, $\mathcal{I}_0$ denotes the modified Bessel function of the first kind of order zero [12] and $\mathbb{E}_\theta[\cdot]$ represents the expectation operator over θ. The original MAP rule can be approximated into two different metrics for $\mathcal{S} \gg \mathcal{I}$ (low-INR region) and $\mathcal{I} \gg \mathcal{S}$ (high-INR region) as described in the following subsections:

A. *Approximate MAP rule for low-INR*

When $\mathcal{S} \gg \mathcal{I}$, the second term in (2) is negligible and the “treat interference as noise” (TIN) decoding rule can be applied in the decoding [3], such as,

$$\arg \min_{k\in\{1,\cdots,M\}} \mathbb{E}_\theta \left[|y - \sqrt{\mathcal{S}}x_k|^2 \right]. \tag{3}$$

B. *Approximate MAP rule for high-INR*

In the case of $\mathcal{S} \ll \mathcal{I}$, the optimal MAP rule can be approximated based on “interference cancellation (IC)” principle, where the decoding rule is expressed as [3]

$$\arg \min_{k\in\{1,\cdots,M\}} \mathbb{E}_\theta \left(|y - \sqrt{\mathcal{S}}x_k| - \sqrt{\mathcal{I}} \right)^2. \tag{4}$$

III. Error Performance Analysis

In order to investigate the error performance of any given convolutionally coded system, the calculation of the transfer function, $T(D, K)$, is the pivotal step. The mostly used transfer function calculation method used in many studies [13] is only valid under the assumption of quasi-regularity. In [14], a general method which can be readily be used for both QR and irregular cases had been proposed as it was reemphasized in [10], [15].

In order to represent the most general error performance analysis with the existence of ARI, the product-state matrix technique in the calculation of $T(D, K)$ is utilized. For a given $T(D, K)$, a BER upper bound [16, (9)] can be calculated as

$$P_b \leq \frac{1}{k} \frac{\partial}{\partial K} T(D, K) \bigg|_{K=1}, \tag{5}$$

where k is the number of information bit(s) per symbol.

For the calculation of $T(D, K)$, it is assumed to have a N-state convolutional encoder and it yields N^2 ordered pairs of product-states (u, v), where u is an actual encoder state in the transmitter and v is a Viterbi decoder's state in the receiver, $(u, v \in \{1, ..., N\})$. Then, $N^2 \times N^2$ product-state matrix $\mathbf{S}(D, K)$ can be constructed with its entries based on transitions from (u, v) to $(\bar{u}, \bar{v})$. Let $D_{(u,v),(\bar{u},\bar{v})}$ denote the branch label for transition $(u \to \bar{u})$ and $(v \to \bar{v})$. It was shown in [17] that each entry of $\mathbf{S}(D, K)$ can then be written as

$$\begin{aligned}[\mathbf{S}(D, K)]_{(u,v),(\bar{u},\bar{v})} &= p(u \to \bar{u}|u) \\ &\times \sum_n p_n K^{a(u\to\bar{u})\oplus a(v\to\bar{v})} D_{(u,v),(\bar{u},\bar{v})},\end{aligned} \tag{6}$$

assuming both transitions $(u \to \bar{u})$ and $(v \to \bar{v})$ exist, otherwise $[\mathbf{S}(D, K)]_{(u,v),(\bar{u},\bar{v})} = 0$. The summation in (6) is over the n possible parallel transitions depending on a given encoder, where p_n denotes the probability of nth parallel transition between $(u \to \bar{u})$ if it exists, otherwise $p_n = 1$. In (6), $p(u \to \bar{u}|u)$ is the conditional probability of transition from state u to state $\bar{u}$ given state u, and $a(u \to \bar{u})$ denotes the Hamming weight of the information sequence for the transition from u to $\bar{u}$ [17]. Using the same notation given in [14], the product-states can be categorized into 'good states' $\mathcal{G}$ where $u = v$ and 'bad states' $\mathcal{B}$ where $u \neq v$. After suitably ordering the product-states, $\mathbf{S}(D, K)$ can be written as [14]

$$\mathbf{S}(D, K) = \begin{bmatrix} \mathbf{S}_{\mathcal{G}\mathcal{G}}(D, K) & \mathbf{S}_{\mathcal{G}\mathcal{B}}(D, K) \\ \mathbf{S}_{\mathcal{B}\mathcal{G}}(D, K) & \mathbf{S}_{\mathcal{B}\mathcal{B}}(D, K) \end{bmatrix}. \tag{7}$$

Using the partitioning in (7), the transfer function in (5) can be calculated as [14]

$$T(D, K) = a + \mathbf{b}^T \left[\mathbf{I} - S_{BB}(D, K) \right]^{-1} \mathbf{c}, \tag{8}$$

where $a = \mathbf{1}^T \mathbf{S}_{\mathcal{G}\mathcal{G}}(D, K) \mathbf{1}$, $\mathbf{b} = \mathbf{1}^T \mathbf{S}_{\mathcal{G}\mathcal{B}}(D, K)$, and $\mathbf{c} = \mathbf{S}_{\mathcal{B}\mathcal{G}}(D, K) \mathbf{1}$. Here, $\mathbf{1}$ and $\mathbf{I}$ denotes a vector of ones and identity matrix, respectively. As it can be seen in (6), each entry of $\mathbf{S}(D, K)$ contains $D_{(u,v),(\bar{u},\bar{v})}$, so in order to calculate average BER bound expression, the transition probabilities in (5) are required. To do so, $D_{(u,v),(\bar{u},\bar{v})}$ for *low-INR* region and *high-INR* region are derived in the following subsections by utilizing the approximated MAP rules given in (3) and (4), respectively.

A. Calculation of $D_{(u,v),(\bar{u},\bar{v})}$ for low-INR region

In the case of $\mathcal{S} \gg \mathcal{I}$, (3) can be applied as the decoding rule in soft-decision Viterbi decoding process. Then, the probability of decoding an erroneous symbol, $\hat{x}$, instead of an actually transmitting one, x, can be formulated as [18]

$$\mathcal{D}_{(u,v),(\bar{u},\bar{v})} = \Pr\left(\left|y - \sqrt{\mathcal{S}}x\right|^2 - \left|y - \sqrt{\mathcal{S}}\hat{x}\right|^2 \geq 0\right). \quad (9)$$

Regarding the product-state indices, $(v \rightarrow \bar{v})$ is an erroneous decoder transition in Viterbi decoder where $(u \rightarrow \bar{u})$ is an actual transition at the transmitter. Now, the performance analysis for low-INR region is represented for different types of constellations as follows:

*1) **M-AM**:* When M-AM constellation is used in the transmitter, $D^{M-\mathrm{AM}}_{(u,v),(\bar{u},\bar{v})}$ can be expressed as

$$\begin{aligned} D^{M-\mathrm{AM}}_{(u,v),(\bar{u},\bar{v})}\left(\mathcal{S},\Delta,\mathcal{I}\right) =& \frac{1}{2}\operatorname{erfc}\left(\sqrt{\frac{\mathcal{S}}{4}}\Delta\right) \\ &+ \frac{2}{\sqrt{\pi}}e^{-\frac{\mathcal{S}}{4}d^2}\mathcal{A}\left(\mathcal{S},\mathcal{I},\Delta,n\right). \end{aligned} \quad (10)$$

Here, $\operatorname{erfc}(\cdot)$ denotes the complementary error function [12] and $\mathcal{A}\left(\mathcal{S},\Delta,n\right)$ can be calculated from

$$\begin{aligned} \mathcal{A}\left(\mathcal{S},\mathcal{I},\Delta,n\right) =& \sum_{n=1}^{\infty}\frac{(-1)^n}{n!}H_{n-1}\left(\sqrt{\frac{\mathcal{S}}{4}}\Delta\right) \\ &\times \frac{\Gamma\left(\frac{1+n}{2}\right)\left(1+(-1)^n\right)^2\mathcal{I}^{n/2}}{2^{1-\frac{n}{2}}n\sqrt{\pi}\Gamma\left(n/2\right)}, \end{aligned} \quad (11)$$

for $\Delta \geq 0$ where $H_{n-1}(\cdot)$ is the Hermite polynomial of order n [12] along with $\Delta = x - \hat{x}$ (see Appendix A for the details). For $\Delta < 0$, $D^{M-\mathrm{AM}}_{(u,v),(\bar{u},\bar{v})}$ can be rewritten as

$$\begin{aligned} D^{M-\mathrm{AM}}_{(u,v),(\bar{u},\bar{v})}\left(\mathcal{S},\Delta,\mathcal{I}\right) =& 1 - \frac{1}{2}\operatorname{erfc}\left(\sqrt{\frac{\mathcal{S}}{4}}\Delta\right) \\ &- \frac{2}{\sqrt{\pi}}e^{-\frac{\mathcal{S}}{4}\Delta^2}\mathcal{A}\left(\mathcal{S},\mathcal{I},\Delta,n\right). \end{aligned} \quad (12)$$

*2) **Squared M-QAM**:* When squared M-QAM is used in the transmitter, the erroneous transition analysis can be derived from after utilizing (10) since a squared M-QAM is the Cartesian product of two identical $\sqrt{M}$-AM constellations. Using this fact, the correct transition probability can be expressed as the product of two correct transition probabilities of $\sqrt{M}$-AM constellation, that is,

$$\begin{aligned} \mathbb{E}_\theta\Big[&\left(1 - \mathcal{Q}\left(\sqrt{\mathcal{S}/4}\Delta_R + \sqrt{2\mathcal{I}}\cos\theta\right)\right) \\ &\times \left(1 - \mathcal{Q}\left(\sqrt{\mathcal{S}/4}\Delta_I + \sqrt{2\mathcal{I}}\cos\theta\right)\right)\Big], \end{aligned} \quad (13)$$

where $\Delta_R = \Re\{x\} - \Re\{\hat{x}\}$ and $\Delta_I = \Im\{x\} - \Im\{\hat{x}\}$. Also, $\Re\{\cdot\}$ and $\Im\{\cdot\}$ represent the real and imaginary parts of complex number, respectively. Then, $D^{M-\mathrm{QAM}}_{(u,v),(\bar{u},\bar{v})}\left(\mathcal{S},\Delta_R,\Delta_I,\mathcal{I}\right)$ can be found in the form of given in (14) at the top of the next page.

*3) **Irregular M-ary**:* In the given previous cases, the signal point locations in a given constellation are restricted to be either in one dimension (M-AM), or on regular lattices, (squared M-QAM). In the case of an irregular M-ary constellation, $\mathcal{D}^{M-\mathrm{ary}}_{(u,v),(\bar{u},\bar{v})}$ can be expressed as

$$\begin{aligned} &\mathcal{D}^{M-\mathrm{ary}}_{(u,v),(\bar{u},\bar{v})}\left(\mathcal{S},\Delta_R,\Delta_I,\mathcal{I}\right) \\ &= \mathbb{E}_\theta\left[\mathcal{Q}\left(\frac{\sqrt{\mathcal{S}}}{2}|\Delta| - \frac{\sqrt{\mathcal{I}}}{|\Delta|}\cos\theta\Delta_R + \frac{\sqrt{\mathcal{I}}}{|\Delta|}\sin\theta\Delta_I\right)\right], \end{aligned} \quad (15)$$

with $|\Delta| = \sqrt{\Delta_R^2 + \Delta_I^2}$. After utilizing [eq.(10), [19]], (15) can be simplified as

$$\begin{aligned} D^{M-\mathrm{ary}}_{(u,v),(\bar{u},\bar{v})}\left(\mathcal{S},\Delta_R,\Delta_I,\mathcal{I}\right) =& \frac{1}{2}\operatorname{erfc}\left(\sqrt{\frac{\mathcal{S}}{8}}|\Delta|\right) \\ &+ \frac{1}{\sqrt{\pi}}e^{-\frac{\mathcal{S}}{8}\Delta^2}\mathcal{B}\left(\mathcal{S},\mathcal{I},\Delta_R,\Delta_I,n\right), \end{aligned} \quad (16)$$

where the definition of the auxiliary function, $\mathcal{B}\left(\mathcal{S},\Delta_R,\Delta_I,\mathcal{I},n\right)$, is given as

$$\begin{aligned} \mathcal{B}\left(\mathcal{S},\Delta_R,\Delta_I,\mathcal{I},n\right) =& \sum_{n=1}^{\infty}\frac{(-1)^n}{n!}H_{n-1}\left(\sqrt{\frac{\mathcal{S}}{8}}|\Delta|\right) \\ \times \left(\frac{\mathcal{I}}{2|\Delta|}\right)^{n/2} & \frac{\left(1+(-1)^n\right)\left(\Delta_I^2+\Delta_R^2\right)^{n/2}\Gamma\left(\frac{1+n}{2}\right)}{2\sqrt{\pi}\Gamma\left(1+n/2\right)}. \end{aligned} \quad (17)$$

B. Calculation of $D_{(u,v),(\bar{u},\bar{v})}$ for high-INR region

In the case of $I \gg \mathcal{S}$, the error analysis is based on the approximated MAP rule given in (4) and as it was shown in [5], this results in an equivalent channel model such that

$$y_{\mathrm{eq}} = \Re\{e^{-j\theta}\sqrt{\mathcal{S}}x\} + Z_{\mathrm{eq}}, \quad (18)$$

with $Z_{\mathrm{eq}} \sim \mathcal{N}\left(0,1/2\right)$. For this equivalent channel, decoding $\hat{r}$ instead of an actually transmitting equivalent symbol, r, $\mathcal{D}_{(u,v),(\bar{u},\bar{v})}$ can be expressed as

$$\mathcal{D}_{(u,v),(\bar{u},\bar{v})} = \Pr\left(\left|y_{\mathrm{eq}} - r\right|^2 - \left|y_{\mathrm{eq}} - \hat{r}\right|^2 \geq 0\right), \quad (19)$$

where $r = \Re\{e^{-j\theta}x\}$ and $\hat{r} = \Re\{e^{-j\theta}\hat{x}\}$.

*1) **M-AM**:* After applying some mathematical manipulations into (19), $D^{M-\mathrm{AM}}_{(u,v),(\bar{u},\bar{v})}$ turns into

$$\mathcal{D}^{M-\mathrm{AM}}_{(u,v),(\bar{u},\bar{v})} = \mathbb{E}_\theta\left[\mathcal{Q}\left(\sqrt{\frac{\mathcal{S}}{2}}\left(r - \hat{r}\right) + \sqrt{2\mathcal{I}}\cos\theta\right)\right]. \quad (20)$$

Then, $D^{M-\mathrm{AM}}_{(u,v),(\bar{u},\bar{v})}$ can be found as

$$\begin{aligned} \mathcal{D}^{M-\mathrm{AM}}_{(u,v),(\bar{u},\bar{v})}\left(\mathcal{S},\Delta,\mathcal{I}\right) =& \frac{\pi^{1/2}}{4} - \left(\Delta\sqrt{\frac{\mathcal{S}}{2}} + \sqrt{2\mathcal{I}}\right) \\ &\times \frac{{}_2F_2\left(\frac{1}{2},1;\frac{3}{2},\frac{3}{2};-\left(\Delta\sqrt{\frac{\mathcal{S}}{2}}+\sqrt{2\mathcal{I}}\right)^2\right)}{\pi}, \end{aligned} \quad (21)$$

where, $\Delta = x - \hat{x}$ and ${}_pF_q\left(\cdot,\cdot;\cdot,\cdot;\cdot\right)$ is the generalized hypergeometric function [12] (see Appendix B for the details).

$$
\begin{aligned}
D^{M-\mathrm{QAM}}_{(u,v),(\bar{u},\bar{v})}\left(\mathcal{S},\Delta_R,\Delta_I,\mathcal{I}\right) &= 1-D^{\mathrm{AM}}_{(u,v),(\bar{u},\bar{v})}\left(\frac{\mathcal{S}}{2},\Delta_I,\mathcal{I}\right)-D^{\mathrm{AM}}_{(u,v),(\bar{u},\bar{v})}\left(\frac{\mathcal{S}}{2},\Delta_R,\mathcal{I}\right)+\frac{1}{4}\operatorname{erfc}\left(\sqrt{\frac{S}{8}}\Delta_I\right) \\
&\operatorname{erfc}\left(\sqrt{\frac{\mathcal{S}}{8}}\Delta_R\right)+\frac{1}{2}\operatorname{erfc}\left(\sqrt{\frac{\mathcal{S}}{8}}\Delta_R\right)\frac{2}{\sqrt{\pi}}e^{-\frac{S}{8}\Delta_I^2}\mathcal{A}\left(\frac{S}{2},\mathcal{I},n_2,\Delta_I\right)+\frac{1}{2}\operatorname{erfc}\left(\sqrt{\frac{\mathcal{S}}{8}}\Delta_R\right)\frac{2}{\sqrt{\pi}}e^{-\frac{S}{8}\Delta_I^2}\mathcal{A}\left(\frac{\mathcal{S}}{2},\mathcal{I},n_1,\Delta_R\right) \\
&+\frac{4}{\pi}e^{-\frac{S}{8}d_R^2+\Delta_I^2}\sum_{n_1=1}^{\infty}\sum_{n_2=1}^{\infty}\frac{(-1)^{n_1+n_2}}{n_1!n_2!}H_{n_1-1}\left(\sqrt{\frac{S}{8}}\Delta_R\right)H_{n_2-1}\left(\sqrt{\frac{S}{8}}\Delta_I\right)\frac{\Gamma\left(\frac{1+n_1+n_2}{2}\right)\left(1+(-1)^{n_1+n_2}\right)^2\mathcal{I}^{n_1+n_2/2}}{2^{1-\frac{n_1+n_2}{2}}n_1+n_2\sqrt{\pi}\Gamma\left(n_1+n_2/2\right)}.
\end{aligned}
\tag{14}
$$

*2) **Squared M-QAM**:* The similar steps already applied for the case of the squared M-QAM over the low-INR region can be followed by using (21).

*3) **Irregular M-ary**:* Considering the equivalent channel model in high-INR region and well-known Chernoff bound, the probability of decoding erroneous transition for an irregular M-ary constellation can be expressed as [20]

$$
\mathcal{D}^{M-\mathrm{ary}}_{(u,v),(\bar{u},\bar{v})}=\mathbb{E}_\theta\left[e^{-|r-\hat{r}|^2/2}\right]=\mathbb{E}_\theta\left[e^{-|\cos\theta\Delta_R+\sin\theta\Delta_I|/2}\right]. \tag{22}
$$

After using the trigonometric identity [Eq. (1.314.11), [12]], which is,

$$
a\cos(\theta)+b\sin(\theta)=\sqrt{a^2+b^2}\cos\left(\theta-\arctan\left(\frac{b}{a}\right)\right) \tag{23}
$$

and utilizing [eq. 3.915.4, [12]], $\mathcal{D}^{M-\mathrm{ary}}_{(u,v),(\bar{u},\bar{v})}$ can be derived as

$$
\mathcal{D}^{M-\mathrm{ary}}_{(u,v),(\bar{u},\bar{v})}\left(\mathcal{S},\Delta_R,\Delta_I\right)=e^{-\mathcal{S}R^2/4}\mathcal{I}_0\left(\mathcal{S}R^2/4\right), \tag{24}
$$

where $R=\sqrt{\Delta_I^2+\Delta_R^2}$ and $\mathcal{I}_n(\cdot)$ is the modified Bessel function of the first kind [12].

C. QR cases

The product-state matrix technique offers the most general error performance analysis for coded systems regardles of the choice of a convolutional encoder and a M-ary constellation. However, it comes at the expense of increased complexity in the analytical calculations. In the QR cases, the complexity of analysis can be reduced considerably by assuming that the all zeros code word is sent by the transmitter where $u\to 0$ and $v\to 0$ in (7). Then, the size of product-state matrix in the QR scenario reduces from $N^2\times N^2$ to $N\times N$. It should also be noted that being QR does not imply better or worse performance and it only brings simplified error performance calculation [17].

IV. Numerical Results

In this section, the derived error performance expressions are validated through the Monte Carlo simulations. In all scenarios considered, the natural bit-to-symbol mapping rule is selected to generate output symbols from encoded bits and soft-decision Viterbi decoding is used along with TIN and IC decoders for low-INR and high-INR regions, respectively. Also, BER curves are plotted with respect to $\mathcal{S}/\mathcal{I}$ values for low-INR region and $\mathcal{I}/\mathcal{S}$ values for high-INR region. Considering the simplicity and its popularity, a rate-1/2 convolutional encoder $[5,7]_8$ is employed in the transmitter along with 4-AM, 4-QAM and irregular 64-ary constellations.

TABLE I: Convergence of (10) with N_c terms for (11).

N_c	$\mathcal{S}/\mathcal{I}=8$ dB, $\mathcal{I}=3$ dB	$\mathcal{S}/\mathcal{I}=14$ dB, $\mathcal{I}=1$ dB
5	−4.61896127305	−7.38431518149
10	−4.91291703902	−6.27283776732
15	−3.9827146718	−6.23620318367
20	−4.11417579146	−6.24976229191
25	−4.11168375519	−6.25029611649
50	**−4.11777939018**	**−6.25027493545**
100	−4.11777939018	−6.25027493545

A. Low-INR region

In order to validate the derived error performance metrics for low-INR region, (10) and (14), we first simulate three different scenarios for 4-AM and 4-QAM constellation cases along with different interference levels such that $\mathcal{I}=\{1,3,5\}$ dB. In the calculation of (10), the infinite summation term seen in (11) is truncated after 50th term since Table I shows the convergence of the infinite summation in (11) for different $\mathcal{S}/\mathcal{I}$ values and $\mathcal{I}$ values and the corresponding log10(P_b) values. Fig. 2 demonstrates that the derived BER bound expression for M-AM and its extension to M-QAM yield good agreement with simulated BER values for higher $\mathcal{S}/\mathcal{I}$ values.

B. High-INR region

Now, the derived error performance analysis for high-INR region, (21), is tested through the simulations. In the simulations, QAM modulation is considered for $\mathcal{S}=10$ dB and $\mathcal{S}=12$ dB, the simulated and analytical BER values are plotted with respect to different $\mathcal{I}/\mathcal{S}$ values. As it can be seen from Fig. 3, the derived bound expression is validated with simulated BER values for both cases.

C. Irregular constellation cases

In order to validate the analysis for an irregular M-ary constellation, (16), irregular 64-ary constellation given in Fig. 4 which was originally proposed in [18] is used and $[1101;0111]$ is also applied as the puncturing pattern in $[5,7]_8$ convolutional encoder. Fig. 5 shows that the derived error bound expression is in good agreement with the simulated results. From this point of view, (16) has considerable potential to be used to find optimized constellations for a given INR value in future research.

V. Conclusions

We presented error performance for a generic, convolutionally coded transmission coexisting with

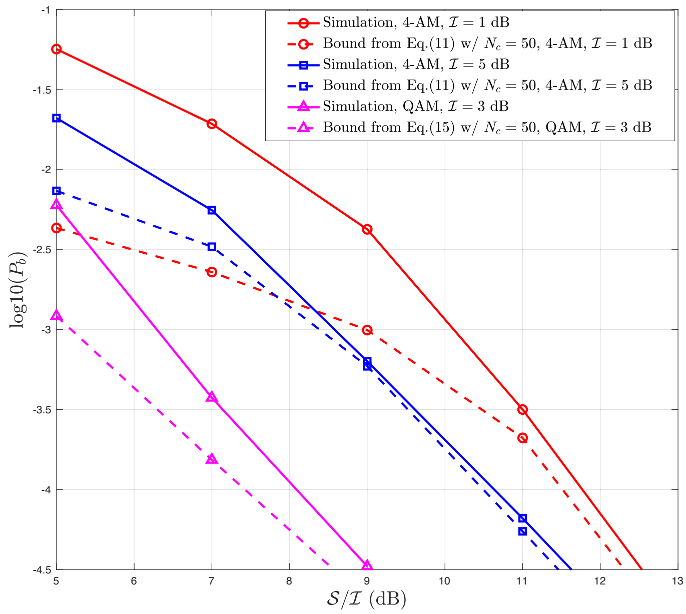

Fig. 2: BER bound validation of $[5, 7]_8$ convolutionally coded system with 4-AM and QAM cases in low-INR region.

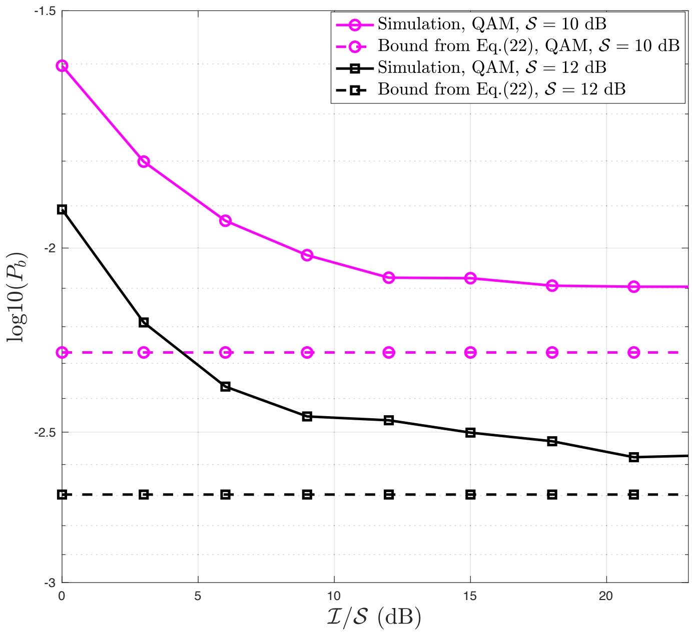

Fig. 3: BER bound validation of $[5, 7]_8$ convolutionally coded system with QAM cases in high-INR region.

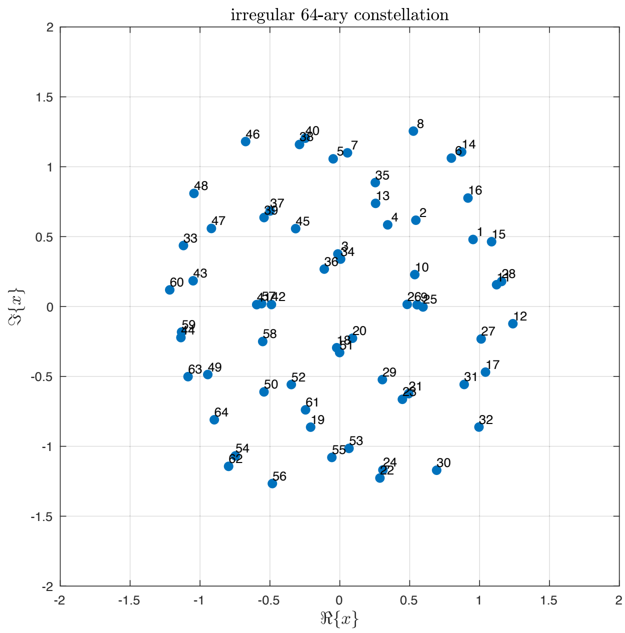

Fig. 4: The constellation diagram of irregular 64-ary constellation.

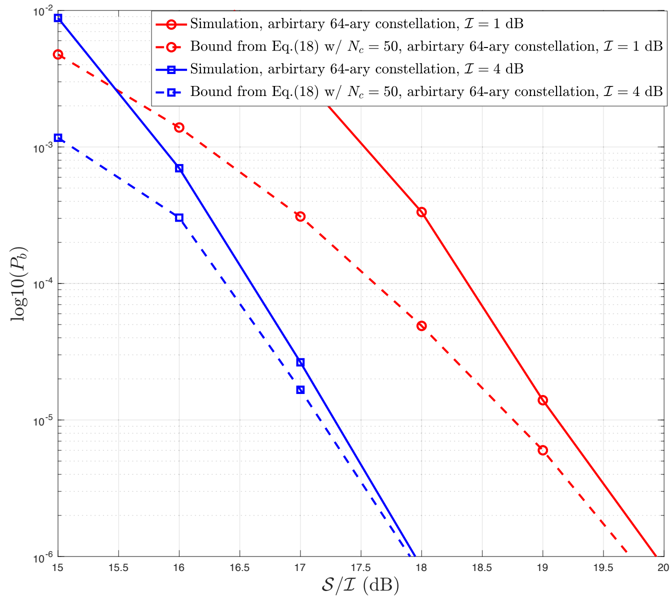

Fig. 5: BER bound validation of $[5, 7]_8$ convolutionally coded system with irregular 64-ary constellation given in Fig.4.

non-cooperative radar interference. The proposed error analysis is compatible with any convolutional encoder and constellation where symbol locations can be completely arbitrary since the product-state matrix technique is utilized. This extends the existing methods which can only be used when the encoder and constellation satisfy the quasi-regularity conditions. These conditions might be violated in the systems where optimized irregular constellations are used to improve performance. In addition, the presented analysis can be extended to the turbo trellis-coded systems to enable the irregular constellation optimization in the presence of more advanced error correcting coding techniques.

Appendix A: Calculation of (11)

The conditional probability of erroneous decoding for a given θ, $\Pr[x \to \hat{x}|\theta]$, can be expressed as

$$\Pr[x \to \hat{x}|\theta] = \Pr\Bigg[\frac{\sqrt{S}}{2}|x - \hat{x}|^2 + \Re\{\sqrt{I}e^{i\theta}(x - \hat{x})^*\} + \Re\{z(x - \hat{x})^*\}\Bigg]. \tag{25}$$

Then, considering $(x-\hat{x}) \in \mathcal{R}$ for M-AM, (25) simplifies to

$$\begin{aligned}\Pr\left[x \to \hat{x}|\theta\right] &= \Pr\left[z^{''} \leq -\sqrt{\frac{S}{2}}\left(x-\hat{x}\right) - \sqrt{2\mathcal{I}}\cos\theta\right] \\ &= \mathcal{Q}\left(\sqrt{\frac{S}{2}}\left(x-\hat{x}\right) - \sqrt{2\mathcal{I}}\cos\theta\right),\end{aligned} \tag{26}$$

where $z^{''} \sim \mathcal{N}(0,1)$. The unconditional $\Pr[x \to \hat{x}]$ can be found as

$$\Pr\left[x \to \hat{x}\right] = \mathbb{E}_{\theta}\left[\mathcal{Q}\left(\sqrt{\frac{S}{2}}\left(x-\hat{x}\right) - \sqrt{2\mathcal{I}}\cos\theta\right)\right]. \tag{27}$$

Then, using the identity of that $\mathcal{Q}(x) = (1/2)\,\mathrm{erfc}\left(x/\sqrt{2}\right)$ and [Eq.(10), [19]], that is,

$$\mathrm{erfc}\left(x+y\right) = \mathrm{erfc}\left(x\right) + \frac{2}{\sqrt{\pi}}e^{-x^2}\sum_{n=1}^{\infty}\frac{(-1)^n}{n!}H_{n-1}\left(x\right)y^n, \tag{28}$$

along with the definition of $\Delta = x - \hat{x}$, $\mathcal{A}(\mathcal{S},\mathcal{I},\Delta,n)$ can be derived as in (11).

APPENDIX B: CALCULATION OF (21)

By using the relation between the Gaussian $\mathcal{Q}$-function and the complementary error function, (20) turns into

$$\begin{aligned}\mathcal{D}^{M-\mathrm{AM}}_{(u,v),(\bar{u},\bar{v})} &= \mathbb{E}_{\theta}\left[\frac{1}{2}\,\mathrm{erfc}\left(\sqrt{\frac{S}{2}}\Delta + \sqrt{2\mathcal{I}}\cos\theta\right)\right] \\ &= \frac{1}{\sqrt{\pi}}\int_{\cos\theta\left(\Delta\sqrt{\frac{S}{2}}+\sqrt{2\mathcal{I}}\right)}^{\infty} e^{-t^2}dt.\end{aligned} \tag{29}$$

Applying the change of integration variable $t \to t^{'}\cos\theta$ into (29) results in

$$\mathbb{E}_{\theta}\left[\frac{1}{\sqrt{\pi}}\int_{\Delta\sqrt{\frac{S}{2}}+\sqrt{2\mathcal{I}}}^{\infty} e^{-t^{'2}\cos^2\theta}\cos\theta dt^{'}\right]. \tag{30}$$

By changing the order of the integrals, (30) can be rewritten as

$$\begin{aligned}&\frac{1}{\sqrt{\pi}}\int_{\Delta\sqrt{\frac{S}{2}}+\sqrt{2\mathcal{I}},\Delta\geq 0}^{\infty}\left\{\int_{\cos\theta\geq 0} e^{-t^{'2}\cos^2\theta}\cos\theta d\theta\right\}dt^{'} \\ &+ \frac{1}{\sqrt{\pi}}\int_{\Delta\sqrt{\frac{S}{2}}+\sqrt{2\mathcal{I}},\Delta< 0}^{\infty}\left\{\int_{\cos\theta< 0} e^{-t^{'2}\cos^2\theta}\cos\theta d\theta\right\}dt^{'}.\end{aligned} \tag{31}$$

With the definition of the Dawson's integral [21], $\mathcal{F}(\cdot)$, the expression simplifies to

$$\begin{aligned}&\frac{1}{\sqrt{\pi}}\int_{\Delta\sqrt{\frac{S}{2}}+\sqrt{2\mathcal{I}},\Delta\geq 0}^{\infty}\frac{\mathcal{F}\left(t^{'}\right)}{t^{'}\pi}dt^{'} + \\ &\qquad \frac{1}{\sqrt{\pi}}\int_{\Delta\sqrt{\frac{S}{2}}+\sqrt{2\mathcal{I}},\Delta< 0}^{\infty} -\frac{\mathcal{F}\left(t^{'}\right)}{t^{'}\pi}dt^{'}.\end{aligned} \tag{32}$$

Then, using [22], (21) can be obtained.

REFERENCES

[1] H. T. Hayvaci and B. Tavli, "Spectrum sharing in radar and wireless communication systems: A review," in *Proc. Int. Conf. IEEE Electromagn. Adv. Appl.*, 2014, pp. 810–813.

[2] B. Paul, A. R. Chiriyath, and D. W. Bliss, "Survey of RF communications and sensing convergence research," *IEEE Access*, vol. 5, pp. 252–270, 2017.

[3] N. Nartasilpa, A. Salim, D. Tuninetti, and N. Devroye, "Communications system performance and design in the presence of radar interference," *IEEE Trans. Commun.*, vol. 66, no. 9, pp. 4170–4185, Sep 2018.

[4] S. Shahi, D. Tuninetti, and N. Devroye, "On the capacity of the AWGN channel with additive radar interference," *IEEE Trans. Commun.*, vol. 66, no. 2, pp. 629–643, Feb 2018.

[5] N. Nartasilpa, D. Tuninetti, N. Devroye, and D. Erricolo, "On the error rate of a communication system suffering from additive radar interference," in *Proc. IEEE Glob. Commun. Conf. (GLOBECOM)*, Dec 2016, pp. 1–6.

[6] F. Brunero, D. Tuninetti, and N. Devroye, "On code design for wireless channels with additive radar interference," arXiv: 1904.05484 [cs.IT], 2019.

[7] M. Shirvanimoghaddam, M. S. Mohammadi, R. Abbas, A. Minja, C. Yue, B. Matuz, G. Han, Z. Lin, W. Liu, Y. Li, S. Johnson, and B. Vucetic, "Short block-length codes for ultra-reliable low latency communications," *IEEE Commun. Mag.*, vol. 57, no. 2, pp. 130–137, Feb. 2019.

[8] C. Rachinger, J. B. Huber, and R. R. Mller, "Comparison of convolutional and block codes for low structural delay," *IEEE Trans. Commun.*, vol. 63, no. 12, pp. 4629–4638, Dec. 2015.

[9] I. Parvez, A. Rahmati, I. Guvenc, A. I. Sarwat, and H. Dai, "A survey on low latency towards 5G: RAN, core network and caching solutions," *IEEE Commun. Surv. Tutorial*, vol. 20, no. 4, pp. 3098–3130, 4thquarter 2018.

[10] M. C. Ilter, P. A. Dmochowski, and H. Yanikomeroglu, "Revisiting error analysis in convolutionally coded systems: The irregular constellation case," *IEEE Trans. Commun.*, vol. 66, no. 2, pp. 465–477, Feb. 2018.

[11] F. Alberge, "Deep learning constellation design for the awgn channel with additive radar interference," *IEEE Transactions on Communications*, vol. 67, no. 2, pp. 1413–1423, Feb. 2019.

[12] I. S. Gradshteyn and I. Ryzhik, *Table of Integrals, Series, and Products*, 7th edition. Academic Press, 2007.

[13] A. Viterbi and J. Omura, *Principle of digital communication and coding*. McGraw-Hill, 1979.

[14] E. Biglieri, "High-level modulation and coding for nonlinear satellite channels," *IEEE Trans. Commun.*, vol. 32, no. 5, pp. 616–626, 1984.

[15] S. Benedetto, M. Mondin, and G. Montorsi, "Performance evaluation of trellis-coded modulation schemes," *Proc. IEEE*, vol. 82, no. 6, pp. 833–855, Jun 1994.

[16] D. Divsalar, M. Simon, and J. Yuen, "Trellis coding with asymmetric modulations," *IEEE Trans. Commun.*, vol. 35, no. 2, pp. 130–141, Feb. 1987.

[17] J. Shi and R. D. Wesel, "Efficient computation of trellis code generating functions," *IEEE Trans. Commun.*, vol. 52, no. 2, pp. 219–227, Feb. 2004.

[18] M. C. Ilter and H. Yanikomeroglu, "Convolutionally coded SNR-adaptive transmission for low-latency communications," *IEEE Trans. Veh. Technol.*, vol. 67, no. 9, pp. 8964–8968, Sep. 2018.

[19] Y. Zhao and S. . Haggman, "BER analysis of OFDM communication systems with intercarrier interference," in *Proc. Int. Conf. on Commun. Technol.*, vol. 2, Oct 1998, pp. 5 pp. vol.2–.

[20] M. K. Simon and M.-S. Alouini, *Digital communication over fading channels*. John Wiley & Sons, 2005, vol. 95.

[21] E. W. Weisstein, "Dawson's integral." *From MathWorld–A Wolfram Web Resource*. [Online]. Available: http://mathworld.wolfram.com/DawsonsIntegral.html

[22] J. Murley and N. Saad, "Tables of the Appell hypergeometric functions F_2," *arXiv preprint arXiv:0809.5203*, 2008.